Stochastic phase portraits of a damped bistable oscillator driven by colored noise

Frank Moss, Peter Hänggi, R. Mannella, P. V. E. McClintock

Stochastic phase portraits of a damped bistable oscillator driven by colored noise

Frank Moss

Department of Physics, University of Missouri at St. Louis, St. Louis, Missouri 63121

Peter Hanggi

Department of Physics, Polytechnic Institute of New York, Brooklyn, New York 11201

R. Mannella and P. V. E. McClintock

Department of Physics, University of Lancaster, Lancaster LA1 4YB, United Kingdom

(Received 21 February 1986)

We present measurements of the stationary, joint statistical densities of velocity and displacement in a three-dimensional system: the damped oscillator with a bistable potential driven by additive, colored noise. Approximate Fokker-Planck theories of such "higher-dimensional" systems are assessed and compared to the measurements. Because of limitations inherent in all present theories and generally available numerical techniques, analog simulators appear to offer the only effective, high-resolution means for obtaining the joint probability densities of $d = 3$ systems.

There has been a great deal of interest in recent years in simple, "archetypal" descriptions of a variety of nonlinear, nonequilibrium, macroscopic phenomena, along with a growing appreciation of the role played by external noise in such systems.[1] One such widely studied archetype is the damped, anharmonic oscillator

$$\ddot{x} + \gamma \dot{x} = -\frac{dU(x)}{dx} + V_n(t) \ , \tag{1}$$

where γ is the damping, $U(x)$ is a potential, and $V_n(t)$ is an additive driving force. When $U(x)$ is a periodic potential, Eq. (1) has been used, for example, as a model for the resistively shunted Josephson junction[2,3] or, in the limit of large damping, the ring-laser gyroscope.[4] When $U(x)$ is a bistable potential, applications too numerous to list in detail range from a driven Ge photoconductor[2] and a nonlinear elastic mechanical oscillator[5] to models of optical bistability.[6,7] $V_n(t)$ can be either aperiodic or periodic, for which in the latter case Eq. (1) has been used to model a number of interesting chaotic systems.[2,5,7]

In this Rapid Communication, we confine the discussion to Eq. (1) with a bistable potential and with $V_n(t)$ a purely aperiodic noise for which there exists no evidence of chaotic behavior. We thus consider the problem of Brownian motion in a double-well potential, first treated by Kramers,[8] and more recently by Risken and his co-workers[9,10] and reviewed by one of us.[11] We present the first measurements of the stochastic phase portraits (SPP's) made on an analog simulator of this system. Studies on a simulator of Eq. (1) with a periodic potential are currently in progress. When V_n is a *time-correlated* noise, the system is three dimensional ($d = 3$):

$$\dot{x} = v \ , \tag{2a}$$

$$\dot{v} = x - x^3 - \gamma v + V_n(t, \tau) \ , \tag{2b}$$

$$\dot{V}_n = -(1/\tau) V_n + \Gamma(t)/\tau \ , \tag{2c}$$

where we have used the bistable potential $U(x) = -x^2/2 + x^4/4$. The noise $V_n(t)$ is exponentially correlated with correlation time τ, as defined by Eq. (2c), with the white noise source $\langle \Gamma(t) \Gamma(s) \rangle = (2D) \delta(t - s)$ of intensity D.

Equations (2) are reducible to a $d = 2$ system in either of two ways. First, in the white-noise limit

$$\dot{x} = v \ , \tag{3a}$$

$$\dot{v} = x - x^3 - \gamma v + V_n(t) \ , \tag{3b}$$

where now $\langle V_n(t) V_n(s) \rangle \propto \delta(t - s)$; or second in the limit of large damping

$$\gamma \dot{x} = x - x^3 + V_n(t, \tau) \ , \tag{4}$$

with V_n again defined by Eq. (2c). A $d = 1$ system is obtained when both limits apply.

Such systems have most often been studied theoretically using an exact or approximate Fokker-Planck (FP) analysis.[12] The FP equation can, however, be solved for the stationary densities exactly and in closed form only for $d = 1$ systems. This is a strong restriction because, while many highly dissipative systems can be accurately modeled in the limit of large damping,[6] it is not likely that any macroscopic system is reasonably modeled in a white-noise limit as, for example, recent experience with dye-laser transitions has demonstrated.[13]

Solutions of higher-dimensional FP equations are afforded by the matrix continued-fraction (MCF) method.[12] The final result is, however, a matrix of infinite dimension which must be truncated and inverted numerically, a necessarily approximate procedure. It turns out that this matrix can be evaluated with sufficient accuracy on computers available to most laboratories (say, a VAX) only for $d = 2$ systems. Even so, for such systems large amounts of processing time (~ 1 h) are required for high accuracy. Digital simulations are beset by similar problems. We have simulated Eqs. (2) on a VAX with results which confirm the major features of the data reported below, but even for long processing times we were unable to resolve the detailed structure. By contrast, as we show below, *measurements* of the stationary joint probability densities $P(\dot{x}, x)$, the SPP's, can be obtained rapidly and simply to accuracies of 10% or less from analog simulators. We have recently demonstrated excellent agreement with the MCF theory of similar measurements of $P(V_n, x)$ for a widely studied $d = 2$ system.[10,14]

MOSS, HANGGI, MANNELLA, AND McCLINTOCK

Of course, approximate theoretical methods for treating non-Markovian FP systems have been known for some time,[15] and have recently been applied to a number of important problems by several groups.[13,16] These methods, valid only in the limits of small D and τ, all rely essentially on a Taylor expansion around the Markovian limit. We have recently pointed out that such approximation schemes fail to predict accurately both the long-time dynamics[17] and the observed renormalization of the shape of $P(x)$ with increasing τ.[18] We have put forth an improved but still approximate scheme, which has been worked out within two different theoretical frameworks[19] and successfully applied to both $d=2$ and $d=3$ systems. We quote here only the result of this recent investigation:[18]

$$P(\dot{x},x) = N[\exp(-\dot{x}^2/2\sigma_v)][\exp(x^2/2 - x^4/4)/\sigma_x] , \quad (5a)$$

with

$$\sigma_x = (D/\gamma)[1 + \tau(3\langle x^2\rangle - 1)/(\gamma + 1/\tau)]^{-1} , \quad (5b)$$

$$\sigma_v = (D/\gamma)[1 + \gamma\tau + \tau^2(3\langle x^2\rangle - 1)]^{-1} . \quad (5c)$$

We note that the τ dependence of σ_x guarantees first that $P(x)$ $[= \int_{-\infty}^{\infty} P(\dot{x},x)d\dot{x}]$ will become narrower and grow in amplitude with increasing τ; and second that, since $\langle x^2\rangle \simeq 1$, the effective diffusion coefficients are always greater than 0. Both these features represent significant improve-

ments on the traditional approximations. However, the new approximation, while accurate for large τ, becomes less so for large D as we show below. In addition, Eq. (5a) is even in both $\dot{x}$ and x, and hence does not predict an interesting asymmetry which is clearly evident in the present, high-resolution measurements for $d=3$.

An electronic circuit, composed entirely of analog components, was designed to mimic Eqs. (2a) and (2b) with a steady-state accuracy of a few percent. The circuit was driven with an additive, time-correlated noise voltage in accord with Eq. (2c), or its equivalent, $\langle V_n(t)V_n(s)\rangle = (D/\tau)\exp[-(t-s)/\tau]$. Noisy output voltages representing velocity $\dot{x}$ and displacement x were digitized into time series from which the two-dimensional stationary densities $P(\dot{x},x)$ were assembled and averaged. The experimental arrangement, accuracy, and measurement techniques have been discussed in greater detail elsewhere[14,18] and so will not be elaborated here.

Figure 1 shows our measurements of $P(\dot{x},x)$, displayed as three-dimensional plots on the left and as contours of constant probability on the right for τ ranging from approximately white ($\tau=0.25$) in Fig. 1(a), to very colored ($\tau=4.0$) noise in Fig. 1(b). The $P(\dot{x},x)$ plots clearly show the narrowing of the peaks and the increasing depth of the valley between with increasing τ, while the contours show the developing asymmetry which tends to skew the valley toward an axis running from lower left to upper right. In
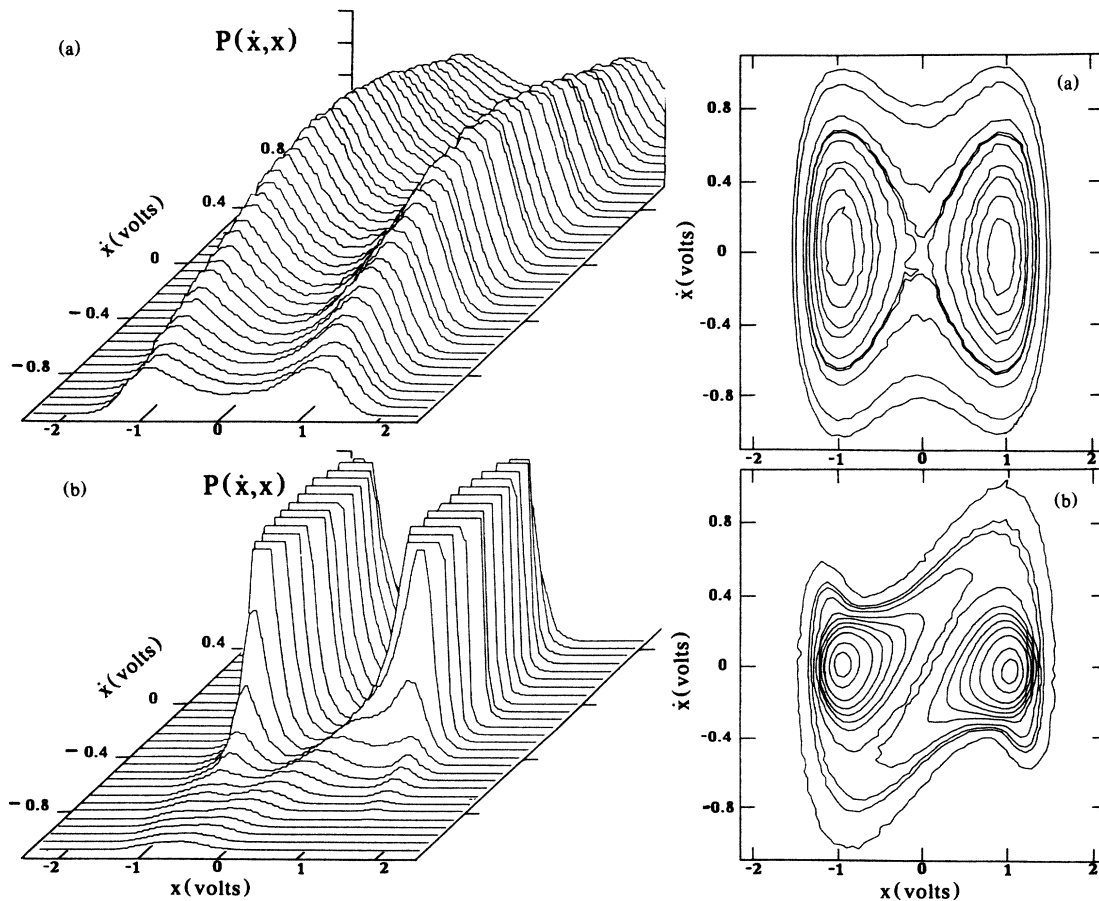

FIG. 1. The measured stochastic phase portraits for $\gamma=1$ and $D=0.3$ and for (a) $\tau=0.25$ and (b) $\tau=4.0$. The vertical scale is arbitrary. The amplitudes of the contours of constant probability vary from (a) 256 to 3.5×10^3 with two contours near the separatrix at $\simeq 1.2\times10^3$ and (b) 512 to 32×10^3 with separatrix at $\simeq 4\times10^3$.

addition, Fig. 1(b) shows the emergence of a third maximum in the $P(x)$ cross sections cut along the x directions at $x \sim 1.2$, $\dot{x} \sim 0.4$ (and $x \sim -1.2$, $\dot{x} \sim -0.4$). It should be noted that this feature was not observed in either the MCF calculations[10] or in the analog simulations[14] of the $d = 2$ system, though the skewing effect was clearly evident. Since the MCF calculations require a supercomputer for $d = 3$, the approximate, analytic theories do not predict any asymmetry, and digital simulations do not yet result in sufficient resolution, it is apparent that, at present, analog simulations offer the only effective means by which SPP's of high enough resolution to detect these novel features can be obtained.

We have also measured the effect of changing the damping γ. Large damping has the effect of restoring the lost symmetry caused by large τ, while increasing the height of the peaks and the depth of the valley. While the latter effect is predicted by the approximate theory [Eq. (5)], the characteristic asymmetric effects are not.

Figure 2 shows our one-dimensional measurements of $P(x)$ and $P(\dot{x})$ (noisy curves) compared to Eqs. (5) (smooth curves) for small noise intensity D and increasing τ in (a)–(b), and for fixed τ but increasing D in (c)–(d). The normalization of the calculated curves was adjusted to match the maxima of the measured results. It is evident that the new approximate theory gives an accurate account of the one-dimensional densities for *surprisingly large* τ but only for $D \lesssim 0.3$. On the contrary, the conventional theories[15,16] exhibit unphysical probability densities (divergencies) for the realistic parameter values used here.

In conclusion, we have obtained the SPP's of Eqs. (2) with unprecedented detail and statistical quality, and we have used them to explore the range of validity of a recently proposed approximation scheme for treating non-Markovian, higher-dimensional systems. Our analog simulation
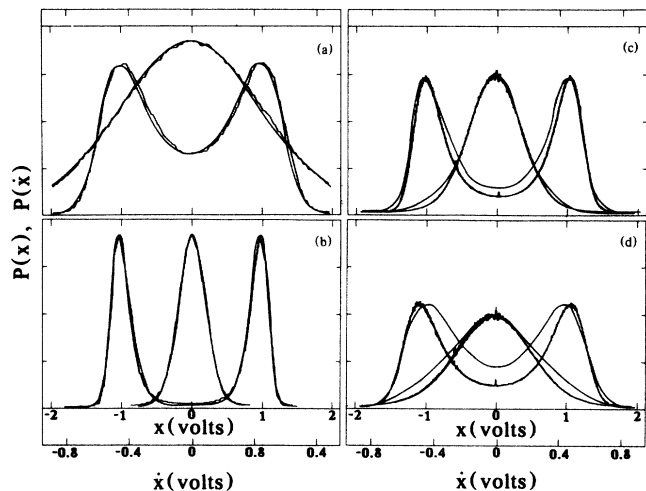

FIG. 2. Measured one-dimensional monomodal densities $P(\dot{x})$, and bimodal densities $P(x)$, shown by the noisy curves compared to Eqs. (5); smooth curves for $\gamma = 1$ and with $D = 0.3$ for (a) $\tau = 0.25$, (b) $\tau = 4.0$; and with $\tau = 2.0$ for (c) $D = 0.5$ and (d) $D = 1.0$. The experimental results in (a) and (b) were obtained from the two-dimensional densities by summing over all values of the other variable; while in (c) and (d), the $1 - d$ densities were measured directly.

techniques may prove useful for studies on other especially intractable systems.

[1]See, for example, *Fluctuations and Sensitivity in Nonequilibrium Systems*, edited by W. Horsthemke and D. K. Kondepudi, Springer Proceedings in Physics, Vol. I (Springer, Berlin, 1984).

[2]E. G. Gwinn and R. M. Westervelt, Phys. Rev. Lett. **54**, 1613 (1985), and references therein; S. W. Teitsworth and R. M. Westervelt, *ibid.* **56**, 516 (1986).

[3]M. Buttiker, E. P. Harris, and R. Landauer, Phys. Rev. B **28**, 1263 (1983).

[4]W. W. Chow, J. Gea-Banacloche, L. M. Pegrotti, V. E. Sanders, W. Schleich, and M. O. Scully, Rev. Mod. Phys. **57**, 61 (1985), and references therein.

[5]F. C. Moon and G.-X. Li, Phys. Rev. Lett. **55**, 1439 (1985).

[6]R. Graham, M. Hohnerbach, and A. Schenzle, Phys. Rev. Lett. **48**, 1396 (1982); F. T. Arecchi, R. Meucci, G. Puccioni, and J. Tredicce, *ibid.* **49**, 1217 (1982).

[7]For a short, but excellent review, see N. B. Abraham, L. A. Lugiato, and L. M. Narducci, Phys. Today **39** (No. 1), S53 (1985).

[8]H. A. Kramers, Physica **7**, 284 (1940).

[9]K. Voigtlaender and H. Risken, J. Stat. Phys. **40**, 397 (1985).

[10]P. Jung and H. Risken, Z. Phys. B **61**, 367 (1985).

[11]P. Hanggi, J. Stat. Phys. **42**, 105 (1986).

[12]H. Risken, *The Fokker-Planck Equation* (Springer, Berlin, 1984).

[13]A. Schenzle and R. Graham, Phys. Lett. **98A**, 319 (1983);

R. Short, L. Mandel, and R. Roy, Phys. Rev. Lett. **49**, 647 (1982); P. Lett, R. Short, and L. Mandel, *ibid.* **52**, 341 (1984); R. F. Fox, G. E. James, and R. Roy, Phys. Rev. A **30**, 2482 (1984); R. Roy, A. W. Yu, and S. Zhu, Phys. Rev. Lett. **55**, 2794 (1985).

[14]F. Moss and P. V. E. McClintock, Z. Phys. B **61**, 381 (1985).

[15]R. L. Stratonovich, *Topics in the Theory of Random Noise* (Gordon and Breach, New York, 1963), Vol. I; M. Lax, Rev. Mod. Phys. **38**, 541 (1966).

[16]N. G. Van Kampen, Phys. Rep. **24C**, 171 (1976); J. M. Sancho, M. San Miguel, S. L. Katz, and J. D. Gunton, Phys. Rev. A **26**, 1589 (1982); K. Lindenberg and B. J. West, Physica A **119**, 485 (1983); **128**, 25 (1984); R. F. Fox, Phys. Lett. **94A**, 281 (1983); L. A. Lugiato and R. J. Harowicz, J. Opt. Soc. **2**, 971 (1985); A. Schenzle and T. Tel, Phys. Rev. A **32**, 596 (1985); R. F. Fox, *ibid.* **33**, 467 (1986).

[17]P. Hanggi, T. J. Mroczkowski, F. Moss, and P. V. E. McClintock, Phys. Rev. A **32**, 695 (1985).

[18]L. Fronzoni, P. Grigolini, P. Hanggi, F. Moss, R. Mannella, and P. V. E. McClintock, Phys. Rev. A **33**, 3320 (1986).

[19]The functional derivative method, Ref. 17, and the projector operator method, Ref. 18.